Short Communication

A cost-effective identification of tobacco alkaloids using porous Si SERS substrates for forensic and bioanalytical applications

Ashish Kumar[1] · Rishi Sharma[1] · Ashok Kumar Sharma[1] · Ajay Agarwal[1]

Received: 10 April 2019 / Accepted: 18 October 2019 / Published online: 26 October 2019

Abstract
With use of surface-enhanced Raman scattering (SERS) substrate, we are able to identify alkaloids of tobacco leaves. First, porous Si arrays were developed using metal-assisted chemical etching and followed by gold (Au) thin layer (50 nm) coating. Au decorated porous Si arrays provide a strong localized electric field and responsible for the enhancement of weak Raman signals of target molecules. Detection of model molecule rhodamine B at low concentration (10^{-9} M) confirmed the SERS activity of the developed substrates. The enhancement factor was calculated to be approximate 10^6. Further, developed substrates were utilized to identify alkaloid in solution of dry tobacco leaves (1 g and 0.25 g) and water (100 Ml). Raman peak 1030 cm^{-1} corresponding to standard nicotine was observed. Understanding of tobacco composition and their Raman vibration mode could be beneficial to decide the biomarker of various diseases related to tobacco chewing and smoking. This work highlights the level free detection of tobacco alkaloids and confirms that Raman spectroscopy technique can utilize for quality control, forensic and bioanalytical analyses of tobacco alkaloids at trace level.

Keywords Porous silicon · Metal assited chemcial etching (MACE) · SERS · Tobacco alkaloids

1 Introduction

Tobacco consumption in human civilization is one of the main causes of death and disease around globally as well as in India. Among the various products of tobacco, smokeless consumption of tobacco is rapidly increasing and turning a serious public health concern. According to the Global Adult Tobacco Survey (GATS) India, 2010, 206 million Indians are habitual to smokeless tobacco/chewing [1]. In spite of government initiative, use of smokeless tobacco is on rise. Smokeless tobacco causes oral cancers, and a number of other cardiovascular diseases [2, 3]. Almost 90% oral cancers are linked to tobacco uses. Available evidences suggest that the rate of mouth cancer is growing among the younger generation. The rise in popularity of tobacco products like Khaini has created a requirement of a rapid method for determining the nicotine or alkaloid content in tobacco products in the field, ideally at the point of sale or identification of early tobacco user.

Identification and detection of single molecule have significant importance in the field of medicine, chemistry, biology and environmental science. For molecular study, Raman spectroscopy is a powerful tool; however, it is limited to dilute solutions of molecule due to a weak Raman scattering signal. Surface-enhanced Raman spectroscopy (SERS) is another variant of Raman spectroscopy in which incoming laser beam interacts with a target molecule in the vicinity of metallic nanostructures. The coupling between the electromagnetic field of light and plasmon resonance of surface metallic nanostructures exhibits significant enhancement in the local field. This local field leads dramatic increment in weak Raman scattering signal [4]. Meanwhile, charge transfer phenomenon among the metal surface and target molecule also contributes in the

✉ Ashish Kumar, ashishvlsi10@gmail.com | [1]Nano Biosensors Group, CSIR-Central Electronics Engineering Research Institute, Pilani, Rajasthan 333031, India.

enhancement of Raman signal [4, 5]. In fact, electromagnetic mechanism plays its vital role in Raman enhancement due to localized surface plasmons.

Since the first introduction of SERS in 1974, it has gained considerable attention of scientific community due to its several advantages and capabilities to sensitive analysis at trace level. The simplest way to fabricate a SERS substrate is to immobilize gold/silver nanoparticles upon a glass substrate. Notwithstanding, distribution of nanoparticles over the planner substrate limits the hotspot density for optimum enhancement.

Many research groups have been demonstrated various SERS substrates based on various substrate materials, i.e., Si nanowires [4, 5], TiO_2 nanorods arrays [6], ZnO nanorods arrays [7] and Ag nanorods arrays [8, 9]. Among all these materials, Si nanostructures/metal geometry shows unique advantage as high reflective index of Si nanoscale concentrate light scattering and gives near field electromagnetic enhancement [10]. SERS intensity enhancement depends on size, shape and dielectric constant of the materials. Therefore, SERS platforms with considerable enhancement have been demonstrated through a number of methods, including laser interference lithography [4], deep UV lithography [11], galvanic displacement reaction [12, 13], e-beam lithography [10, 11] and evaporation (or magnetron sputtering) [14, 15]. However, these methods are time consuming, complicated and not applicable to large scale production [16, 17]. Moreover, uniformity and reproducibility of SERS devices are highly critical for the effective use of SERS in commercial applications. A comparative alternative simple, facile and cost-effective method is need of the hour.

Herein, we utilized metal-assisted chemical etching (MACE) for the development of porous Si. MACE is a strong candidate for realization of porous Si at low cost, simple equipment and low temperature with high throughput. Au thin film was deliberately deposited on porous Si to produce strong localized surface plasmon resonance to boost Raman intensity of analytes. Furthermore, the detection of rhodamine (RhB) at low concentration (10^{-9} M) was demonstrated and confirmed the SERS activity of the developed SERS substrates and followed by identification of Alkaloids in tobacco leaves.

2 Experimental detail

2.1 Development of porous Si

Porous silicon was developed using electroless metal deposition methods based on galvanic cell process. Prior to etching, p-type Si boron doped (resistivity 1–10 Ω-cm) was thoroughly cleaned in tri-chloro ethylene (TCE), acetone and isopropanol to remove impurities or dust particles and followed by HF dipped to remove any native oxide. Cleaned Si substrates were dipped in solution containing HF and $AgNO_3$ for one minute at room temperature to deposit Ag nanoparticles (Ag NPs). Further, Ag NPs decorated samples were kept for etching in an etching solution containing HF and H_2O_2. Etched substrates were transferred in HNO_3 acid to dissolve Ag particles present on the etched sample. Finally, etched samples were rinsed with de-ionized water and dried in nitrogen purging.

2.2 SERS active platform preparation

In order to meke SERS active platform, developed porous Si substrates were decorated with gold nanoparticles thickness (≈ 50 nm) by RF-sputtering system. Since the surface of etched substrates was too rough, islands of gold were formed instead of thin film, it was confirmed by continuity test using multimeter. Gold coated SERS substrates offer an inherent advantage of stability over silver coated surfaces as silver makes oxide in atmosphere.

2.3 Samples preparation

In order to examine the SERS functionality of Au coated porous Si and tobacco alkaloids detection, first of all developed substrates were tested using model molecules of rhodamine B (RhB) and calculated the enhancement factor of the platforms. The Au coated samples were submerged in rhodamine solutions of various concentration (10^{-9} M, 10^{-6} M and 10^{-3} M) for 5 min and rinsed thoroughly. Now the samples were ready to capture the Raman spectra of rhodamine on SERS active platforms. For tobacco alkaloids examination, powder of natural tobacco leaves was arranged from the village where people use to smoke daily. Different masses of tobacco leaves in (0.25 g, and 1 g) were mixed with 100 Ml volume of DI water and prepared uniform solution for 10 minutes. Final solutions were cleaned using filter and utilized to examine tobacco alkaloids using developed SERS substrates as previously discussed.

3 Characterization method

A scanning electron microscope was used to observe the surface and morphology of porous Si and gold coated SERS platforms. Raman measurements were carried out on a Renishaw Raman spectroscopy system at room

temperature, using 785 nm lasers as an excitation power 30 mW. The exposure time was placed 10 s for all samples. The spectroscopic spectra were recorded in the range of 550–1800 cm^{-1}.

4 Results and discussion

4.1 Surface morphology of porous Si

Figure 1a, b shows SEM images of porous Si. Figure 1a clearly revealed that the well-ordered dense and uniform porosity was observed over entire surface. The depth of etched Si was recorded to be approx. 8 µm which is comparatively too much for effective SERS phenomenon [18]. Though, long wires provide more surface area for hotspot formation, adsorption of target molecules and SERS enhancement. However, increment of light trapping in the structures prevents the collection of SERS signal from the target molecules. Therefore, an optimized etch depth of porous Si arrays is necessary to balance the hot spot density and light trapping. The mechanism for the development of porous Si is well documented in literature [19, 20]. Au coated Si nanowire is shown in Fig. 1b. SEM images clearly show the uniform etching of Si and coating of Au over the porous Si at low scale. Further, presence of gold on porous Si is confirmed by energy-dispersive X-ray spectroscopy in Fig. 1c.

To characterize the SERS response of gold coated porous Si, Raman spectra were collected by spreading the different concentrations (1 nM to 1 mM) of rhodamine B (RhB) over the developed SERS platforms. The size of the SERS substrate was 1 cm × 1 cm, obtained from Au coated porous Si. The recorded spectra of RhB are shown in Fig. 2. Various vibration modes of RhB compound were observed around 1646, 1510, 1350, 1283, 1192, 1075, 750 and 620 cm^{-1}. The Raman peaks at 1646,

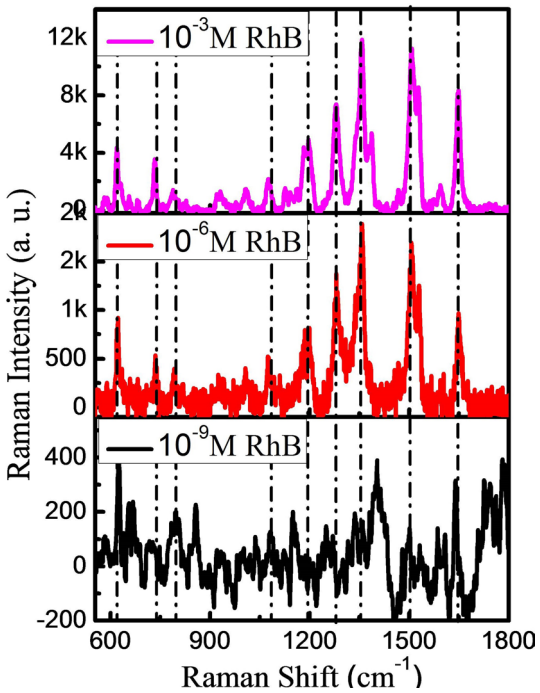

Fig. 2 SERS spectra of rhodamine B (RhB) for different concentrations (10^{-3} M, 10^{-6} M and 10^{-9}M)

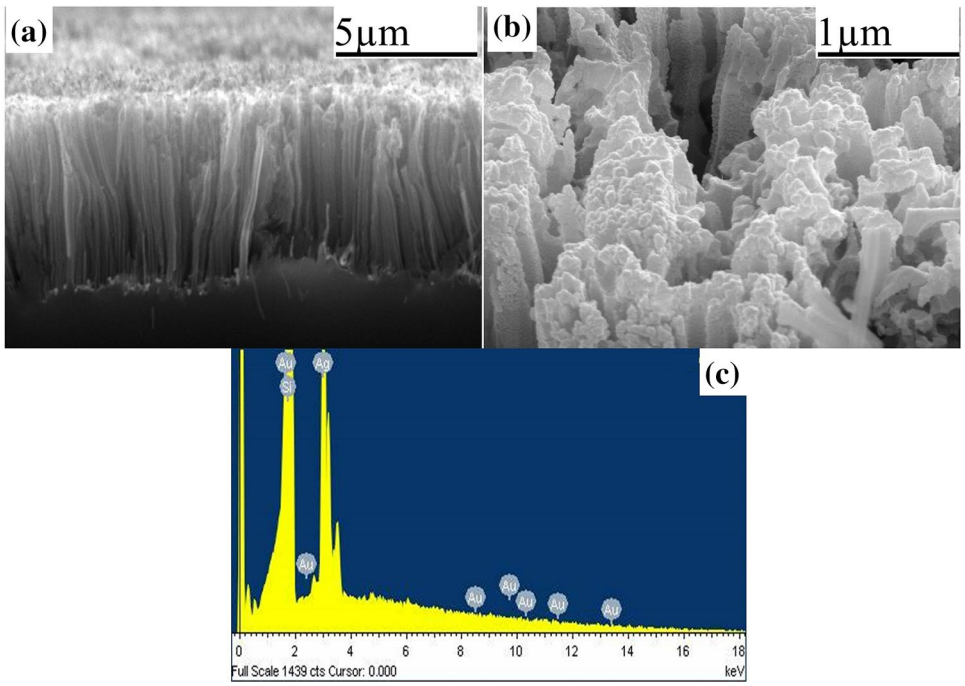

Fig. 1 SEM images etched porous Si **a** cross-sectional view, **b** Au coated porous Si, **c** EDS spectra of Au coated porous Si reveals the presence of Au

1510, 1350 and 620 cm^{-1} are attributed to xanthenes ring stretching of C–C stretching. While bands at 1192, 1075, 750 cm^{-1} and 1193 cm^{-1} are assigned to C–H stretching in methyl group and C–H bending and N–H bending in diethylamino group, respectively [21].

Figure 2 also reveals variation in intensity counts of RhB Raman signal. Intensity counts increase as the concentration of molecule increases. The highest intensity count was observed to be 12,000 counts for Raman band 1350 cm^{-1} of 10^{-3} M RhB samples. At low concentration, the intensity counts drastically decreased around the five fold as the concentration change 10^{-6} M from 10^{-3} M and same order was followed for further decrement in concentration (10^{-9} M) of RhB. The lowest intensity count was 200 for 750 cm^{-1} peak at 10^{-9} M RhB. Though, background noise affects Raman signal at low value of target molecules, Raman intensity peaks of RhB (10^{-9} M) were able to recognize. Here, it is mentioned to worth that the intensity peaks 620, 750 and 1646 cm^{-1} at low concentration (10^{-9} M) were quite matched with the prominent peaks of rhodamine at high concentration and confirmed developed SERS platform is capable to detect molecule at trace level. These results confirmed that developed SERS substrates were uniform and reproducible.

The efficiency of SERS substrate is presented in term of enhancement factor. The simple and qualitative analytical view of enhancement factor was calculated as [22, 23]

$$AEF = \frac{I_{SERS}}{C_{SERS}} \frac{C_R}{I_R}$$

where I_{SERS} and I_R are the intensities of the SERS and Raman signals, respectively, and C_{SERS} and C_R are the concentrations of the analytes in the SERS and control Raman experiments, respectively. The SERS enhancement factor is calculated by comparing the SERS signal excited the RhB adsorbed on the SERS platform and the Raman signal of bulk RhB in control measurement. For AEF measurement, intensity of rhodamine RhB peak (~1350 cm^{-1}) measured in SERS experiment from an aqueous solution (10^{-9} M) of RhB was compared with control Raman measurement of bulk RhB without SERS substrate. The enhancement factor was calculated to be approximate 10^6 for the developed SERS platforms.

Further, developed substrates were utilized for the detection of alkaloids in tobacco leaves. For this, the prepared solution of tobacco leaves in different quantities (1 and 0.25 g) with DI water was dispersed over the SERS active platforms and let the samples dry in atmospheric conditions. The dry samples were scanned to capture Raman spectra of tobacco alkaloids. The recording conditions to capture Raman spectra for the tobacco analysis were kept same as for the RhB in previous experiments.

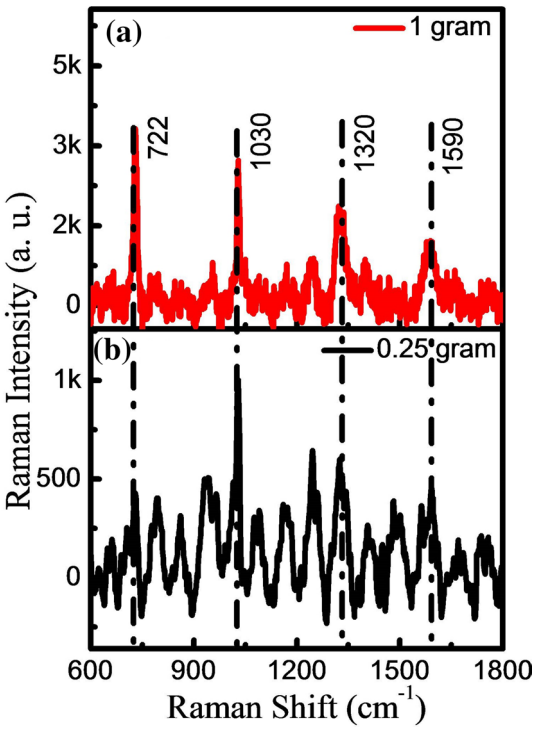

Fig. 3 SERS spectra of tobacco solution in different quantity **a** 1 g, **b** 0.25 g in DI water (100 ml)

The Raman spectra of tobacco mixture are shown in Fig. 3a, b for different concentrations. The more prominent Raman peaks were observed around 722, 1030, 1320 and 1590 cm^{-1} in recorded spectra of 1 g tobacco solution in Fig. 3a. Other than significant peaks, many small peaks were also observed for scanning results, but we focus only significant peaks to study in details. Tobacco alkaloids: nicotine which is named after the *Nicotiana tabacum* L. plant [24] has Raman signature peak at 1030 cm^{-1}. The observed peaks can be assigned to various alkaloids of nicotine divided mainly in two types nicotine-trans-1 or nicotine-trans-2. These types are further categories in term of chiral arrangement of C–C bond and components. The peaks 1030 cm^{-1} assign to free and protonated pyridine moiety vibrations [25]. This Raman signal is perfect matched with well-established Raman signal for nicotine 1030 cm^{-1} using standard nicotine molecule. The peak at 722 cm^{-1} indicates the deformation of pyridine ring while peak 1590 represents the stretching in C–N ring. The peak corresponding to 1320 might assign to C–H bending vibration, yet to confirm in detail study. Almost similar spectrum was observed for 0.25 g tobacco solution in DI water in

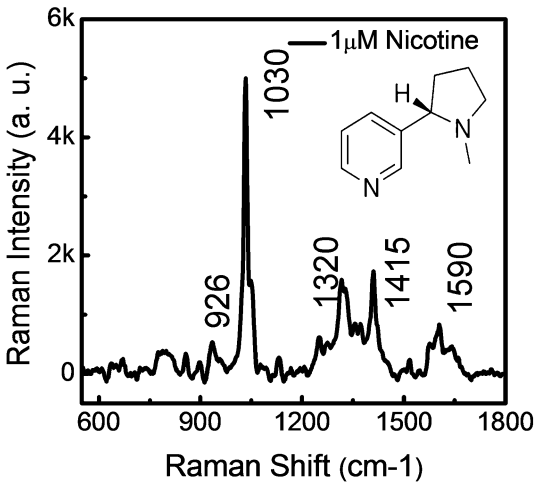

Fig. 4 Raman spectrum of standard nicotine solution (1 μM) and Inset image shows nicotine structures

Fig. 3b. However, intensity of peaks significantly reduced. Here, it is worth to mention that Raman peak 1030 cm^{-1} corresponding to C–C bond in nicotine molecule is quite distinguishable at low value of tobacco in DI water.

Further to confirm the tobacco alkaloid in tobacco leaves, the recorded spectra were compared with Raman spectrum of standard nicotine molecule. Standard solution of nicotine molecule was purchased from Sigma-Aldrich with standard molarity 6.23 M. From this standard solution, a diluted solution (1 μM) of Nicotine was prepared for testing the Raman spectra and recorded spectrum is shown in Fig. 4. The most prominent peak 1030 cm^{-1} along with 1320 and 1590 cm^{-1} was observed and resembled the similar peaks of tobacco solution. Additional peaks 926 and 1415 cm^{-1} could be assign to trans-nicotine conformers [24]. This Raman shift also appear is the Raman spectra of tobacco Fig. 3a, but intensity counts are not so significant. Another explicit remark from Fig. 4 is the absence of 722 cm^{-1} Raman shift as appeared in Raman spectra of tobacco solution. The presence of 722 cm^{-1} peak indicates the deformation of pyrrolidine ring nicotine molecule which could be possible in tobacco solution [24]. Pyridine is most stable in nicotine molecule and could be responsible for the absence of 722 cm^{-1} Raman shift in Raman spectra of standard molecule. Similar results were also recorded from the old sample of tobacco when Raman scanning was done after 5 days. That indicates ingredient of tobacco decompose and get stable nicotine molecule. The recorded Raman spectra of old tobacco sample were similar to standard nicotine sample as shown in Fig. 4. For similar value of concentration, experiment was performed on SERS active substrate on different location of the substrates, all time intensity counts were obtained almost the same. This confirms the uniform distribution of hot spot on porous Si.

5 Conclusion

In summary, ordered and uniform porous Si was developed by a cost-effective MACE process at room temperature and utilized for SERS application with enhancement factor approximate 10^6. In porous structures, abundant hot spots were formed and electromagnetic coupling occured due to closely separated nano-gap and responsible for the enhancement. The substrate was effectively demonstrated the detection of rhodamine molecule at low concentration (10^{-9} M) as well as tobacco alkaloids in the solution of tobacco (1 g and 0.25 g) and water (100 mL). The Raman spectra of tobacco alkaloids were confirmed with Raman spectrum of standard nicotine molecule. The developed substrates showed uniform intensity. This fabrication process of SERS platform is very cheap and viable option for large scale production of SERS substrates. Therefore, the platforms are applicable to determine nicotine content at wide scale at the point of sell tobacco product and early identification of tobacco user. Further, developed SERS platforms can be utilized for forensic and bioanalytical analysis as per the requirment.

Acknowledgements Authors thank the Process Technology group of CSIR-CEERI Pilani for providing facilities for the fabrication of devices. A. Kumar is grateful to Director, CSIR-CEERI support to carry out this research work. A. Kumar also acknowledges Mr. Prem Kumar, CSIR-CEERI for SEM characterization facility. A. Kumar is thankful to Dr. Kulwant Singh, Associate professor, Department of ECE, Manipal University, Jaipur, for his valuable discussion and suggestion. Authors would also like to thanks CSIR, India for their support through the funding of health mission project HCP0012.

Compliance with ethical standards

Conflict of interest On behalf of all authors, the corresponding author states that there is no conflict of interest.

Statement of human and animal rights Research does not involve human participants and/or animals.

References

1. Global Adult Tobacco Survey (GATS) report, India, 2010
2. Asthana S, Labani S, Kailash U, Sinha DN, Mehrotra R (2018) Association of smokeless tobacco use and oral cancer: a systematic global review and meta-analysis. Nicotine Tob Res 21(9):1162–1171
3. Critchley JA, Unal B (2004) Is smokeless tobacco a risk factor for coronary heart disease? A systematic review of epidemiological studies. Eur J Cardiovasc Prev Rehabilit 11(2):101–112

4. Yang J, Li JB, Gong QH, Teng JH, Hong MH (2014) High aspect ratio SiNW arrays with Ag nanoparticles decoration for strong SERS detection. Nanotechnology 25:465707
5. Lu R, Sha J, Xia W, Fang Y, Gu L, Wang Y (2013) A 3D-SERS substrate with high stability: silicon nanowire arrays decorated by silver nanoparticles. CrystEngComm 15:6207–6212
6. Zhao X, Zhang W, Peng C, Liang Y, Wang W (2017) Sensitive surface enhanced Raman scattering of TiO_2/Ag nanowires induced by photogenerated charge transfer. J Colloid Interface Sci 507:370–377
7. Sinha G, Depero LE, Alessandri I (2011) Recyclable SERS substrates based on Au-coated ZnO nanorods. ACS Appl Mater Interfaces 3:2557–2563
8. Graña SG, Pérez Juste J, Alvare Puebla RA, Martínez AG, Marzán LM (2013) Self assembly of Au @ Ag nanorods mediated by Gemini surfactants for highly efficient SERS active. Supercrystals Adv Opt Mater 1:471–477
9. Zhu C, Meng G, Zheng P, Huang Q, Li Z, Hu X, Wang X, Huang Z, Li F, Wu N (2016) A hierarchically ordered array of silver-nanorod bundles for surface-enhanced Raman scattering detection of phenolic pollutants. Adv Mater 28(24):4871–4876
10. Cui H, Li S, Deng S, Chen H, Wang C (2017) Flexible, transparent, and free-standing silicon nanowire SERS platform for in situ food inspection. ACS Sens 2:386–393
11. Dinish US, Yaw FC, Agarwal A, Olivo M (2011) Development of highly reproducible nanogap SERS substrates: comparative performance analysis and its application for glucose sensing. Biosens Bioelectron 26:1987–1992
12. Bai F, Li M, Fu P, Li R, Gu T, Huang R, Chen Z, Jiang B, Li Y (2015) Silicon nanowire arrays coated with electroless Ag for increased surface-enhanced Raman scattering. APL Mater 3:056101
13. Kara SA, Keffous A, Giovannozzi AM, Rossi AM, Cara E, D'Ortenzi L, Sparnacci K, Boarino L, Gabouze N, Soukane S (2016) Fabrication of flexible silicon nanowires by self-assembled metal assisted chemical etching for surface enhanced Raman spectroscopy. RSC Adv 6(96):93649–93659
14. Li DW, Zhai WL, Li YT, Long YT (2014) Recent progress in surface enhanced Raman spectroscopy for the detection of environmental pollutants. Microchim Acta 181:23–43
15. Mandal S, Erickson D (2008) Nanoscale optofluidic sensor arrays. Opt Express 16:1623–1631
16. Srichan C, Ekpanyapong M, Horprathum M, Eiamchai P, Nuntawong N, Phokharatkul D, Danvirutai P, Bohez E, Wisitsoraat A, Tuantranont A (2016) Highly-sensitive surface-enhanced raman spectroscopy (sers)-based chemical sensor using 3d graphene foam decorated with silver nanoparticles as sers substrate. Sci Rep 6:23733
17. Nguyen BH, Nguyen VH, Tran HN (2016) Rich variety of substrates for surface enhanced Raman spectroscopy. Adv Nat Sci Nanosci Nanotechnol 7:033001
18. Gervinskas G, Seniutinas G, Hartley JS, Kandasamy S, Stoddart PR, Fahim NF, Juodkazis S (2013) Surface enhanced Raman scattering sensing on black silicon. Annalen der Physik 525(12):907–914
19. Xia W, Zhu J, Wang H, Zeng X (2014) Effect of catalyst shape on etching orientation in metal-assisted chemical etching of silicon. CrystEngComm 16:4289–4297
20. Kumar A, Agrawal J, Sharma AK, Singh V, Agarwal A (2019) A cost-effective and facile approach for realization of black silicon nanostructures on flexible substrate. J Mater Sci Mater Electron 30(17):16554–16561
21. Coluccio ML, Das G, Mecarini F, Gentile F, Pujia A, Bava L, Tallerico R, Candeloro P, Liberale C, De Angelis F, Di Fabrizio E (2009) Silver-based surface enhanced Raman scattering (SERS) substrate fabrication using nanolithography and site selective electroless deposition. Microelectron Eng 86:1085–1088
22. Langer J, Aberasturi D, Aizpurua J, Puebla RA, Auguié B, Baumberg JJ, Bazan GC, Bell SE, Boisen A, Brolo AG, Choo J (2019) Present and future of surface enhanced Raman scattering. ACS Nano. https://doi.org/10.1021/acsnano.9b04224
23. Liu Y, Xu S, Li H, Jian X, Xu W (2011) Localized and propagating surface plasmon co-enhanced Raman spectroscopy based on evanescent field excitation. Chem Commun 47(13):3784–3786
24. Baranska M, Dobrowolski JC, Kaczor A, Lipska KC, Górz K, Rygula A (2012) Tobacco alkaloids analyzed by Raman spectroscopy and DFT calculations. J Raman Spectrosc 43:1065–1073
25. Barber TE, List MS, Haas JW, Wachter EA (1994) Determination of nicotine by surface-enhanced Raman scattering (SERS). Appl Spectrosc 48:1423–1427